Strain-stiffening Hydrogels with Dynamic, Secondary Crosslinking

K. P. Sonu[a§], Le Zhou[b§], Santidan Biswas[c], John Klier[d], Anna C Balazs[c], Todd Emrick [b], and Shelly R. Peyton[a]**

[a]Department of Chemical Engineering, University of Massachusetts, 240 Thatcher Way, Life Sciences Laboratory N531, Amherst, Massachusetts 01003, United States

[b]Polymer Science and Engineering Department, University of Massachusetts Amherst, 120 Governors Drive, Amherst, Massachusetts 01003, United States

[c]Chemical Engineering Department, University of Pittsburgh, Pittsburgh, Pennsylvania, 15261, United States

[d]Department of Chemical, Biological and Materials Engineering, University of Oklahoma, Carson Engineering Center, Rm 107, Norman, Oklahoma, 73019-0631, United States.

KEYWORDS: cryptic crosslinks; zwitterion; lipoic acid; phosphorylcholine; biomaterial.

ABSTRACT: Hydrogels are water-swollen, typically soft networks useful as biomaterials and in other fields of biotechnology. Hydrogel networks capable of sensing and responding to external perturbations, such as light, temperature, pH, or force, are useful across a wide range of applications requiring on-demand crosslinking or dynamic changes. Thus far, although mechanophores have been widely described as strain-sensitive reactive groups, embedding this type of force-responsiveness into hydrogels is unproven. Here, we synthesized multi-functional polymers that combine a hydrophilic zwitterion with strong, permanently crosslinking alkenes and dynamically crosslinking dithiols. From these polymers, we created hydrogels that contained irreversible and strong thiol-ene crosslinks and reversible dithiol crosslinks, and they stiffened in response to strain, increasing hundreds of kPa in modulus under compression. We examined variations in polymer composition and used a constitutive model to determine how to balance the number of thiol-ene vs. dithiol crosslinks to create maximally force-responsive networks. These strain-stiffening hydrogels represent potential biomaterials that benefit from the mechano-responsive behavior needed for emerging applications in areas such as tissue engineering.

1. Introduction

Hydrogels are crosslinked polymer networks capable of imbibing large amounts of water. These typically soft materials are increasingly popular in biology and biomedical engineering, with applications ranging from tissue engineering to drug delivery to in vitro cell culture platforms, owing to their biocompatibility, hydrophilicity, and mechanical tunability.[1–3] With respect to this last point, the modulus of hydrogel values can be manipulated via crosslinking density, the strength of crosslinks, and the molecular weight of the backbone polymers.[4] However, over time and particularly when subjected to deformation, hydrogels lose their structural integrity and ultimately fail.[5] In contrast, networks from biological polymers, such as collagen and fibrin, are force-responsive and show rapid strain-stiffening behavior, which is one method by which tissues adapt to stress and strain and maintain integrity over an organism's lifetime.[6–9] Incorporating this feature into synthetic hydrogels would enhance their performance as they adapt to settings that involve dynamic stiffening.

Recently, advances have been made in synthesizing dynamic hydrogels from synthetic starting materials that can be triggered to crosslink after initial casting via light, heat, pH, or enzymes.[10–21] We saw a need to expand upon these stimuli-driven mechanisms to devise systems that were energy-efficient because they could function in dark environments, and temperature-sensitive settings and without using a second component. This was our inspiration for examining mechanical force as a potential crosslinking stimulus. Initial efforts to induce mechano-responsiveness into chemical reactions have demonstrated that some molecular architectures anchored along a polymer chain can undergo chemical reactions when subjected to mechanical force.[22] Such molecules are called mechanophores, and they have been exploited to initiate gelation from a polymer solution.[23] In the case of fully formed hydrogels, strain-induced

stiffening has been demonstrated transiently using systems where polymer extension and packing result from mechanical loading.[24–28] Another strategy is to insert mechanophores into polymer networks.[29,30] When force is applied to the mechanophores, they undergo chemical reactions that further crosslink the polymer chains, thereby strengthening the network. Unfortunately, the force required to activate mechanophores is very high and has a side effect of chain scission and subsequent degradation of networks.[31,32] We sought here to create a network that could stiffen under strain, permanently, under relatively mild forces.

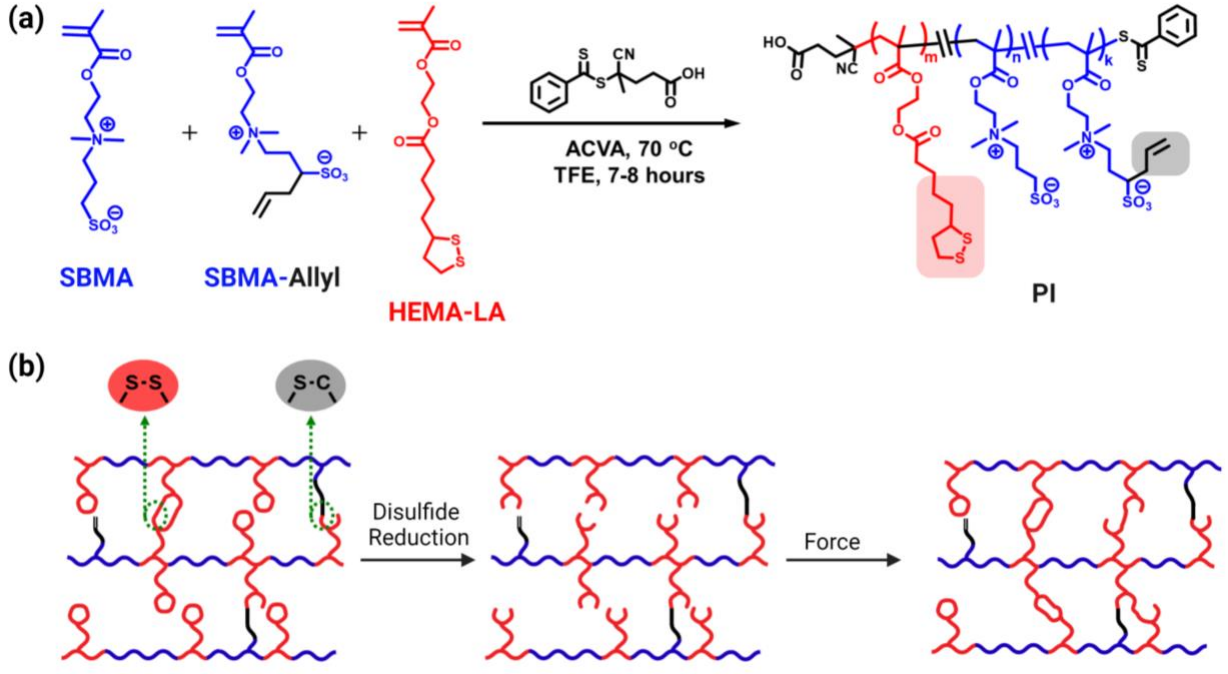

Figure 1. (a) Synthesis of functionalized polymer zwitterions with RAFT polymerization. (b) Schematic illustration of zwitterionic hydrogel network formed through covalent (C-S) and dynamic covalent (S-S) crosslinking. The disulfide reduction of the network generates free thiol groups that form additional crosslinking under cyclic strain and stiffen the network.

Recently, we reported the synthesis of an organogel with mechano-responsive polymer networks containing sterically hindered crosslinking sites, i.e., "cryptic gels".[33] Building on this concept, we present hydrogels that combine sulfobetaine polymer zwitterions with 1,2-dithiolanes and allyl as pendent groups on a single polymer chain (**Figure 1a**). The strained cyclic disulfide of the 1,2-dithiolanes donates greater thiol-disulfide exchange relative to conventional systems[34,35] and opens opportunities to prepare dynamic, self-healing structures.[35–37] Moreover, the hydrophilic nature of the polymer zwitterion allows for embedding high concentrations of allyl groups while maintaining hydrophilicity. The polymer crosslinking via the thiol-ene "click" reaction produces a network where strain- stiffening is facilitated by interchain disulfide bonds (**Figure 1b**). We anticipate such functional hydrogels will be useful for applications that require mechano-responsive, hydrophilic, dynamic strengthening networks with precise control over gel modulus.

2. Experimental Section

2.1 Materials.

Acetonitrile (ACN) (anhydrous, 99.8%), 4,4′-azobis(4-cyanovaleric acid) (98%, ACVA), 4-cyano-4-(phenylcarbonothioylthio)pentanoic acid (>97%, CPPA), 2-(dimethylamino)ethyl methacrylate (DMAEMA) (98%), [2-(Methacryloyloxy)ethyl]dimethyl-(3-sulfopropyl) ammonium hydroxide (95%, SBMA), allyl bromide (99%), n-butyllithium (2.5 M in hexanes), lithium phenyl-2,4,6-trimethylbenzoylphosphinate (≥ 95%, LAP), and anhydrous dichloromethane (≥ 99.8%, DCM) were purchased from Sigma Aldrich. 2,2,2-trifluoroethanol (TFE) were purchased from Oakwood Chemical. TFE-d3 and D_2O were purchased from Cambridge Isotope Laboratories. 4-Methoxyphenol (MEHQ) and 4-dimethylaminopyridine (99%, DMAP) were purchased from Acros Organics. Diethyl ether, tetrahydrofuran (THF),

methanol, sodium chloride, tris(2-carboxyethyl)phosphine hydrochloride (TCEP-HCl), 1-ethyl-3-(3-dimethylaminopropyl) carbodiimide hydrochloride (EDC), triethylamine were purchased from Fisher Scientific. LD-alpha-lipoic acid (99.0+%) was purchased from TCI Chemicals. Tetrahydrofuran (THF) was distilled over sodium/benzophenone.

2.2 Instrumentation.

NMR spectra were acquired on a Bruker Avance-500 machine (500 MHz for ^{1}H and 126 MHz for ^{13}C). Gel permeation chromatography was operated at 40 °C using 20 mM sodium trifluoroacetate in TFE as eluent at a flow rate of 1 mL/min on an Agilent 1200 series system equipped with an isocratic pump, an autosampler, Polymer Standards Service (PSS) PFG guard column (8 × 50 mm), three PSS PFG analytical linear M columns (8 × 300 mm, particle size 7 μm), refractive index (RI) detection, and calibration against PMMA standards. GPC samples were filtered through a 0.45 μm PTFE filter prior to analysis. Rheology experiments are performed on an AR2000 parallel plate rheometer (TA Instruments, USA).

2.3 Monomers synthesis.

Synthesis of 2-hydroxyethyl methacrylate-lipoic acid (HEMA-LA). HEMA-LA was prepared according to previously reported procedures.[36] Briefly, lipoic acid (4.00 g), 2-hydroxyl ethyl methacrylate (2.50 g), EDC (4.14 g) and DMAP (0.10 g) were added to 120 mL DCM in a three-neck round bottom flask. The reaction was stirred for 10 hours at room temperature, and the reaction was passed through a plug of basic alumina. DCM was removed by rotary evaporation and vacuum drying to give HEMA-LA (5.20 g) as yellow liquid in 85% yield.

Synthesis of 1-((2-(methacryloyloxy)ethyl)dimethylammonio)hex-5-ene-3-sulfonate (Allyl-SBMA). Allyl-SBMA was synthesized over two steps as reported previously.[38] Briefly, 1,3-propane sultone (4.27 g) was dissolved in THF (120 mL) and the solution was kept at −78 °C. n-

Butyllithium (2.5 M, 18 mL) was dropwise added over 30 min, and the mixture was stirred for an hour, after which allyl iodide (3.10 mL) was added to the reaction mixture. The mixture was stirred at −78 °C for two hours, then the cooling bath was removed, and water was added. The crude product was obtained by extracting the mixture with ethyl acetate (3x), and the combined organic phase was dried over anhydrous $MgSO_4$, and the solvent was removed by rotary evaporation. 3-Allyl-1,2-oxathiolane 2,2-dioxide (2.86 g, ~52%) was obtained as a colorless liquid after column chromatography on silica gel, eluting with ethyl acetate: hexanes mixtures. 3-Allyl-1,2-oxathiolane 2,2-dioxide (2.70 g), DMAEMA (3.4 mL) and MEHQ (0.02 g) were added to acetonitrile (15 mL), and the mixture was stirred at 70 °C for 12 hours. The white solid precipitate was collected by centrifugation and washed with diethyl ether to afford allyl-SBMA (4.3 g) as white solid ~80% yield.

2.4 Representative polymer synthesis.

Polymers **P-12**, **P-26**, **P-31**, and **P-0,** containing 12, 26, 31, and 0 mol% of alkene groups, respectively, and 25 mole % of HEMA-LA incorporation were prepared by reversible addition-fragmentation chain-transfer (RAFT) polymerization of SBMA, SBMA-allyl, and HEMA-LA monomers. For example, for **P-31**, SBMA (1.5 g), allyl-SBMA (1.5 g), HEMA-LA (1.1 g), CPPA (0.064 g), ACVA (0.01 g) and TFE (8 mL) were added to a 25 mL round bottom flask, and the solution was purged with N_2 (g) for ~20-25 minutes. The solution was then stirred at 70 ^oC for 7-8 hours. The polymerization was terminated by removing the heat source and exposing the reaction mixture to air. ^1H NMR spectroscopy in 0.2 M NaCl D_2O (performed on aliquots taken from the reaction mixture) was used to estimate monomer conversion by integrating monomer olefin signals against polymer resonances from 0.5-2.5 ppm, 3.8-4.6 ppm and 5.7 ppm. A monomer conversion of ~80-90% was typically obtained for this polymerization. The solution

was precipitated into 35 mL methanol, and the precipitate was separated by centrifugation and redissolved in TFE. The precipitate was washed with methanol twice, then with diethyl ether. The final precipitate was dried *in vacuo* to provide **P-31** (3 g) in 75% as pink solid (typical yield ~65-80%).

2.5 Hydrogel preparation.

225 mg of **P-12, P-26**, or **P-31** polymer was dissolved in 410 µL 0.2 M $NaCl_{(aq)}$ and the polymer solution was incubated with 45 mg TCEP-HCl at 37 ºC for 2 hours, then ~2-3 mg LAP and 45 µL triethylamine(added to neutralize the solution for dissolving LAP) was added to the solution, which was transferred to the cylindrical silicone molds with the diameter of 5 mm and the height of 5 mm. The solution was exposed to 365 nm UV for 2 hours, affording transparent and colorless hydrogels. The hydrogels were washed and equilibrated with 0.2 M $NaCl_{(aq)}$ before further experiments and characterizations. For **P-0** hydrogels, 225 mg of **P-0** was dissolved in 450 µL 0.2 M $NaCl_{(aq)}$, to which 2,2′-(ethylenedioxy)diethanethiol was added. The solution was heated at 70 ºC for 12 hours, resulting in the formation of **P-0** hydrogels.

2.6 Experimental determination of elastic modulus.

The hydrogel was placed between the parallel plates of a rheometer (TA Instruments, USA) to perform compressive stress-strain mechanical measurements. The hydrogel was compressed by moving the top-plate at a rate of 20 µm/s in air and the initial linear region (0- 5 %) of stress-strain curve was used to determine the elastic moduli. The cross-sectional area of the hydrogels was determined by using the digital caliper (Fisherbrand™ Traceable™) of ±0.03 mm accuracy.

2.7 Strain-induced stiffening of hydrogels.

The hydrogel was taken from the reduction solution right before the mechanical conditioning. The hydrogel was placed in a petri-dish containing 0.2 M $NaCl_{(aq)}$ to avoid drying. The petri-dish with hydrogel was placed between the parallel plates for rheometer. The top-plate was lower such that the hydrogel was confined between the bottom of the petri-dish and top-plate. Compression and tension cycles are performed at 20 μm/s with 0-20 % strain. At pre-determined time intervals, the hydrogel was taken out of the petri-dish, water around the hydrogel was gently removed by Kim wipes, and a single stress-strain measurement was performed "in the air." Please note that the single stress-strain experiment only takes about 40 seconds, and the hydrogel remains fully swollen during the measurement. The elastic modulus of the hydrogel at a given time point was determined from the linear region of the stress-strain curve. Once this measurement was complete, the hydrogel was quickly placed back in the solution, and the cyclic strain was continued.

Additional detailed methods are provided in Supporting Information.

3. Results and Discussion

3.1 Synthesis of functionalized polymer zwitterions.

The polymer zwitterions were synthesized using reversible addition-fragmentation chain-transfer (RAFT) polymerization of [2-(methacryloyloxy)ethyl]dimethyl-(3-sulfopropyl)ammonium hydroxide (SBMA), HEMA-LA (**Figure S1**) and SBMA-Allyl (**Figure S2**) monomers. Successful incorporation of the allyl and dithiolane groups into the copolymers was confirmed by ^{1}H and ^{13}C NMR spectroscopy (**Figure S3a-c**). Copolymers **P-12, P-26,** and **P-31** were synthesized with varying amounts of allyl groups to investigate their impact on hydrogel mechanics. Holding HEMA-LA approximately constant at 22-24 mole percent, allyl-SBMA mole percent values of 12 (**P-12**), 26 (**P-26**), and 31 (**P-31**) were employed and

confirmed by integration of ^{1}H NMR spectral resonances at 5.70, 2.56- 3.25, and 0.47-2.44 ppm (**Figure S3a**). The monomer ratios incorporated into the polymer structures corresponded closely with the feed ratios employed (**Table 1**). The polydispersity index (PDI) (i.e., Mw/Mn) of the polymers broadened with allyl-SBMA content (**Figure S3d**), likely due to the involvement of some pendent alkenes in the propagation mechanism, which becomes increasingly likely at higher alkene content.[38,39]

Table 1: Summary of polymer characterization

Polymers	Alkene:LA:SB (mol%)[a]	M_n (kDa)[b]	PDI[b]
P-12	12:23:65	21.2	1.39
P-26	26:22:52	24.6	1.97
P-31	31:24:45	24.7	2.08
P-0	0:25:75	16.6	1.09

[a]Calculated from ^{1}H NMR signal integration. [b]Obtained by GPC analysis using trifluoroethanol as eluent (with 0.02 M sodium trifluoroacetate).

For comparative analysis, zwitterionic copolymer containing only dithiolane moieties (**P-0**) were also prepared. The ^{1}H NMR spectrum of **P-0** shows 25 mol% inclusion of HEMA-LA from the integration of resonances at 3.87-4.56 ppm and 0.58-2.35 ppm (**Figure S4**). Interestingly, **P-0** showed the lowest PDI among all the polymers, reiterating the interference of alkene groups in the chain propagation process.

3.2 Preparation of hydrogels from functional polymer zwitterions.

Hydrogels **P-12, P-26,** and **P-31** were prepared from polymers by photo-crosslinking them under reducing conditions. As shown in **Figure 2a**, colorless, transparent hydrogels were

prepared in cylindrical molds. All the formulations gave robust hydrogel materials, with the strength observed to be commensurate with the extent of alkene functionality that is responsible for setting the network structure (**Figure 2b, Figure S5a**). Specifically, **P-12** hydrogels had an elastic modulus of 45 ± 2.6 kPa, while **P-26** and **P-31** were significantly stronger, with measured values of ~209 ± 10 kPa and ~350 ± 25 kPa, respectively. Interestingly, the swelling ratio of these hydrogels showed only modest differences despite the large difference in their moduli (**Figure S5b**). This is likely due to the relatively similar zwitterion content across all conditions, which has the largest effect on water swelling.[40] Using rubberlike elasticity theory,[41,42] the theoretical shear modulus of these gels was found to be higher than our observed values, possibly due to loop formation[43] as well as incomplete consumption of alkenes (**Figure S5d**). The mesh size described by Canal-Peppas[44–46] was determined for these hydrogel networks, which showed a dependence on allyl content in the polymer employed. This relation agrees with their respective moduli values. Hydrogels formed from **P-12** showed the largest mesh size of about 1.7 ± 0.1 nm and the mesh size decreased as elastic modulus increased (**Figure S5c**). These linear relationships suggest that the primary network is predominantly produced via thiol-ene crosslinks. Further, the hydrogel remained intact, with a slight, but statistically significant, decrease of elastic modulus (**P-12**, **P-26**, and **P-31**), when we subjected them to chemical reduction (**Figure 2b**), which would presumably break any dithiol crosslinks. These data suggest that network formation does indeed contain some inter-chain dithiol crosslinks between unique HEMA-LA molecules, with the majority of the network formed through thiol-ene crosslinks.

P-0 was crosslinked using the bifunctional thiol 2,2' -(ethylenedioxy)diethanethiol, resulting in opaque hydrogel containing only disulfide crosslinks. Notably, these hydrogels underwent complete sol-gel transition when reduced with TCEP-HCl, while hydrogels made from **P-12, P-**

26, and **P-31** (containing C-S crosslinks) remained intact. Inclusion of both the reactive allyl and dithiolane groups on the polymer backbone promoted gelation of **P-12, P-26,** and **P-31** in an aqueous environment, and the presence of both sulfide and disulfide crosslinking units enables the network to maintain mechanical strength even after disulfide cleavage.

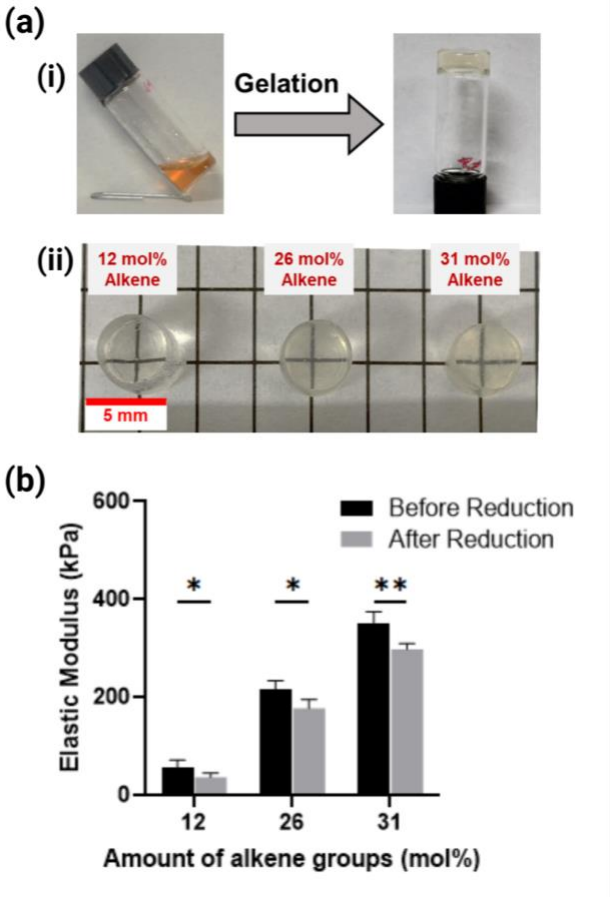

Figure 2. (a) Photographs showing (i) the sol-gel transition from polymer solution to hydrogel network and (ii) hydrogels synthesized in a cylindrical mold for cyclic compression experiments; (b) The elastic modulus of the as synthesized hydrogels before and after chemical reduction. Data represent mean ± SD from N ≥ 3 independent replicates. P-values <0.05 are considered significant, where $p < 0.05$ is denoted with *, and ≤0.01 with **.

3.3 Strain-stiffening Behavior of P-12, P-26, and P-31 Hydrogels.

In evaluating the dynamic nature of the hydrogels, we envisioned the availability of the thiols to provide a mechanically tunable dynamic secondary network through interchain disulfide crosslinks. Following ~ 12 hrs of chemical reduction, the hydrogel was immersed into 0.1 M H_2O_2 to reform disulfides oxidatively (**Figure S6**). In the oxidative environment, the elastic modulus of the hydrogel increased over time (measured around 90-minute intervals) (**Figure 3b-d, Figure S8** and **Figure S10a**). The rate at which this crosslinking occurred was influenced by the initial stiffness of the hydrogel. The weaker hydrogel (**P-12**) showed a minimal increase of elastic modulus (ΔE) i.e., ~14 ± 0.7 kPa increase in 6 h compared to the fully reduced state. **P-12** also had the largest mesh size (1.7 ± 0.1), which suggests most of the thiols reverted to the 1,2-dithiolanes rather than participate in crosslinking (**Figure S7**).[47] In contrast, **P-26** and **P-31** hydrogels, with smaller mesh size, showed much larger increases in ΔE, ~110 ± 8 kPa and ~120 ± 12 kPa, respectively, compared to the corresponding fully reduced state.

In addition to spontaneous stiffening, **P-12, P-26,** and **P-31** hydrogels showed accelerated stiffening in response to cyclic compressive strain due to the increased probability for interchain disulfide bond formation. To study this effect, the hydrogel was subjected to continuous cyclic compression of 20% strain at a rate of 20 μm/s in 0.1 M H_2O_2(aq). ΔE, monitored at around 45 min intervals under compression, increased minimally for **P-12** hydrogels but significantly for **P-26** and **P-31** (**Figure 3b-d, Figure S9** and **Figure S10b**). Notably, the strain-induced conditions led to much greater modulus relative to the unstrained samples. For **P-26**, ΔE increased up to ~371 ± 25 kPa, or nearly three-fold that of the unstrained system. **P-31**, on the other hand, increased to 475 ± 27 kPa under strain. In addition, when **P-26** hydrogel was subjected to a smaller strain (~ 10 %), it still showed stiffening but smaller changes in the modulus compared to hydrogel under 20 % strain (**Figure S11**). The elastic modulus of the stiffened hydrogels

returned to their respective initial values when subjected to chemical reduction (**Figure S12**), which indicate that the interchain disulfide bonds cause the strain-stiffening. To further show that strain-stiffening originates from interchain crosslinking, we subjected **P-26** hydrogels to 20 % strain without the initial chemical reduction step (**Figure S13**), in which case the hydrogel did not stiffen due to the lack of free thiols.

The alkene incorporation of the polymers determined the mesh size of the initial hydrogels, and further effected the rate of change and maximum magnitude of ΔE in the strain stiffening process. After gelation via thiol-ene, two types of free thiols remaining include 1,3-thiols that form thiolane rings[47] and those that are positioned gamma to C-S sulfide units (**Figure 3a**). The higher alkene incorporation in **P-26** and **P-31** led to greater amount of the later type of thiols, whereas for **P-12**, more 1,3-thiols prone to reverting to dithiolanes are left (**Figure S7**). Therefore, the free thiols in **P-26** and **P-31** are more likely to form interchain disulfide crosslinks than that in **P-12**. In addition, the smaller mesh size due to the initial higher crosslink density of **P-26** and **P-31** increased the probability of the interchain disulfide formation. Overall, the thiols that are amenable to interchain crosslinking and the smaller mesh size collectively contribute to the observed faster and larger increase of ΔE values for **P-26** and **P-31** hydrogels under the compressive strain. Interestingly, when the absolute elastic modulus values of **P-26** and **P-31** under strain are scaled to their respective initial modulus (**Figure S10d**), we found **P-31** showed comparable increase of modulus as **P-26** for the first hour under strain, after which **P-26** showed higher evolution over time. This crossover can be ascribed to higher existing crosslinking in **P-31** hydrogel which limits further crosslinking compared to **P-26**.

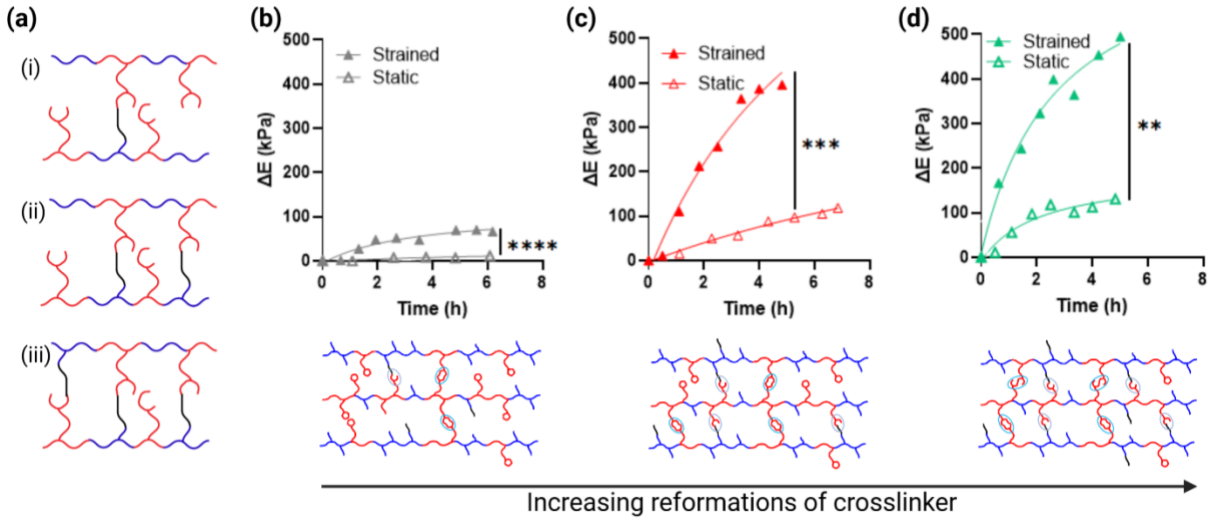

Figure 3. (a) Schematic depiction of 1,3-thiols and thiols that are positioned gamma to C-S sulfide units in (i) **P-12**, (ii) **P-26** and (iii) **P-31** hydrogel networks. Change in Young's modulus ΔE over time post-reduction of different gel structures with or without ~ 20 % cyclic compressive forces for (b) **P-12** (c) **P-26** and (d) **P-31**. Below each curve show the schematic of possible network structure of strained hydrogels. Data represent mean ± SD from N ≥ 2 independent replicates. P-values <0.05 are considered significant, where $p < 0.05$ is denoted with **, ≤0.001 with ***, and ≤0.0001 with ****.

3.3 Theoretical modeling of strain stiffening hydrogels.

In **Figure 3**, although **P-12** has the highest concentration of free thiols, the gel does not exhibit a high modulus due to a large number of dynamic bonds, but rather behaves quite differently. The experimental observation of how strongly the initial network influenced the strain-stiffening behavior was surprising. We use the phenomenological model to better understand the experimental results and elucidate the dynamics. We modified our previously developed

constitutive model to examine the mechanical characteristics of these functional hydrogels.[48,49] The model considered a permanently crosslinked, swollen polymer network that encompasses loops as well as dangling chains that represent secondary crosslinking sites which has been modified to a permanently crosslinked gel with grafted reactive secondary crosslinking sites (**Figure S14**). This model is adapted to systems **A**, **B**, and **C** in **Table S1**, which possess different permanent crosslinks densities (representing C-S bonds) and secondary crosslinks (which capture disulfide reversibility) that correspond to hydrogels **P-13**, **P-26**, and **P-31**, respectively.

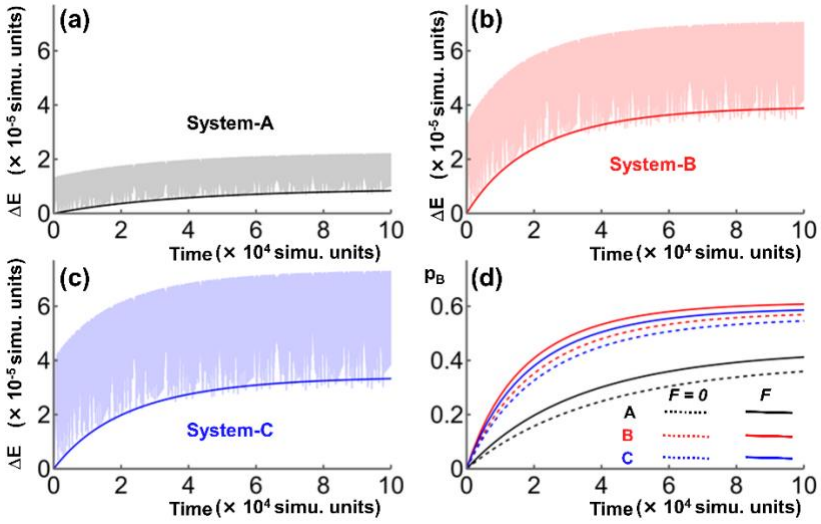

Figure 4. Change in Young's moduli (ΔY) versus time for system (a) **A** (black), (b) **B** (red), and (c) **C** (blue). The lighter colors show the modulus as a function of time in the presence of oscillatory compressive strain. The solid line represents the equilibrium modulus as a function of time, as temporary crosslinks are formed in the absence of any force. d) The probability of binding for the three systems as a function of time in the presence of the compressive force (solid lines) and absence of force (dashed lines).

The model is first employed to evaluate the equilibrium behavior for the three different gel compositions depicted. The volume fraction is consistent with systems to reflect the composition of networks **P-12**, **P-26**, and **P-31**. We compared the initial state of each system, where only C-S bonds are crosslinked, to the fully crosslinked state in which both C-S and S-S bonds are formed at equilibrium. The calculations indicate that swelling of the systems at the initial state decreased with increasing crosslinking density (**Figure S15a**), similar to experimental results (**Figure S5b**). The introduction of secondary S-S crosslinks slightly reduced the swelling degree in all systems. Further, the model is used to calculate the equilibrium elastic moduli (**Figure S15b**), which also show agreement with the experimental observations (**Figure 2b**). Together, these calculations indicate the capability of the model to recapitulate hydrogel structure and properties.

The strain-dependent response of the hydrogels to vibratory deformation is evaluated in the computational model. It is assumed that the deformation rate is sufficiently slow, such that the hydrogel attains the equilibrium degree of swelling instantaneously. Thus, the numerical calculations ignore the relative strain tensor,[48,50] and assume that the dynamics only depends on the instantaneous strain. The compressive strain was modeled using the following equation:

$$\lambda(t) = \lambda_0\left(1 - \left|\lambda_{pct} \times sin\left({}^{2\pi t}/_{T}\right)\right|\right) \qquad (1)$$

where λ_0 is the equilibrium degree of swelling of the hydrogel in the absence of temporary crosslinks. λ_{pct} is the maximum compression applied along the direction of deformation; this value was chosen to be 20%, in line with the experiments. The parameter *t* denotes the period of the compressive strain and was taken to be 240 simulation units, comparable to the protocol used in the experiments (with two-minutes compression cycles). A sinusoidal compressive force with a maximum strain at 20% of the equilibrium extension was applied to each of the systems in line

with the experiments. The temporal changes of Young's modulus brought by the formation of secondary crosslinking (under strain and no strain conditions are evaluated for systems **A**, **B**, and **C** (**Figures 4a-c**). For all systems, the increase of modulus under strain lies above that of the equilibrium state. At $t = 0$, systems contain only permanent crosslinks. As secondary crosslinks (disulfides) form over time, under compression, the degree of secondary crosslinking is higher compared to the no-force scenario, resulting in stiffer hydrogels with higher modulus values. As the concentration of available crosslinks for system **A** was quite low, (recall our assumption that only 50 percent of the available secondary crosslinkers in system A can participate in secondary crosslinking), it can be observed from **Figure 4d** that the fraction of secondary crosslinking is quite low in system **A** for both no force (dashed) and under compression (solid black line) scenario in comparison to system **B** (red) and **C** (blue). As a result, the modulus of hydrogel system **A** is lowest). The probability of binding in systems **B** and **C** are higher than **A**, hence the change in modulus with time under compression is large compared to **system A**. This behavior indicates that the degree of crosslinking (both primary and secondary) governs the stiffening of the hydrogel systems.

4. Conclusion

In this work, novel functional zwitterionic polymers containing both 1,2-dithiolanes and alkene moieties were used to prepare hydrogels with dynamic networks responsive to redox conditions and mechanical force. In our polymer design, the utilization of hydrophilic allyl functionalized SBMA endows aqueous solubility even when significant amounts of allyl groups are present. This unique, bifunctional design imparts gel-formation capability without need for an external

crosslinker. By appropriately tuning the reaction conditions, two types of crosslinking processes (permanent or dynamic) occur. The combination of permanent and dynamic crosslinks gives rise to the types of strain-stiffening features observed for example in the extracellular matrix of tissue. Under static conditions, the crosslinks associated with the permanent network (C-S bonds) define the mechanical state of the initial network and inhibit additional interchain (S-S) crosslinking. However, under cyclic strain, enhanced rates of disulfide crosslinking produce markedly greater stiffening of the network. Importantly, the rate of stiffening is not proportional to the availability of the free thiols but rather to mesh size of the primary network as defined by the permanent crosslinks. We corroborated these experimental observations with computational modeling that provide a better understanding of the strain-stiffening properties and aid future modifications and performance optimizations. The zwitterionic composition and strain-stiffening mechanics make these hydrogels potential biomaterials.

ASSOCIATED CONTENT

Supporting Information.

The following file is available free of charge.

Details of materials and instrumentations used, experimental procedures for the synthesis of monomers, polymers and hydrogels, spectroscopic data, rheological raw data, and details of theoretical calculations. (PDF)

AUTHOR INFORMATION

Corresponding Authors

Todd Emrick - Polymer Science and Engineering Department, University of Massachusetts Amherst, 120 Governors Drive, Amherst, Massachusetts 01003, United States; http://orcid.org/0000-0003-0460-1797; Email: tsemrick@umass.edu

Shelly R. Peyton - Department of Chemical Engineering, University of Massachusetts, 240 Thatcher Way, Life Sciences Laboratory N531, Amherst, Massachusetts 01003, United States; https://orcid.org/0000-0002-7364-8727; Email: speyton@umass.edu

Authors

K. P. Sonu - Department of Chemical Engineering, University of Massachusetts, 240 Thatcher Way, Life Sciences Laboratory N531, Amherst, Massachusetts 01003, United States; https://orcid.org/0000-0003-4450-6014

Le Zhou - Polymer Science and Engineering Department, University of Massachusetts Amherst, 120 Governors Drive, Amherst, Massachusetts 01003, United States

Santidan Biswas - Chemical Engineering Department, University of Pittsburgh, Pittsburgh, Pennsylvania, 15261, United States; https://orcid.org/0000-0002-9204-7820

John Klier - Department of Chemical, Biological and Materials Engineering, University of Oklahoma, Carson Engineering Center, Rm 107, Norman, Oklahoma, 73019-0631, United States

Anna C Balazs - Chemical Engineering Department, University of Pittsburgh, Pittsburgh, Pennsylvania, 15261, United States; https://orcid.org/0000-0002-5555-2692

Author Contributions

K.P.S and L.Z. contributed to drafting the manuscript, data collection, and data interpretation. S.B., and A.C.B contributed to the theoretical modeling. S.B., and J.K. contributed to data analysis and interpretation, and editing the manuscript. T.E., and S.R.P. contributed to conceptual design, data interpretation, and drafting the manuscript. § K.P.S. and §L.Z. contributed equally to this paper.

Funding Sources

Research reported in this publication was supported by the Army Research Office Award Number: W911NF1910388 and National Science Foundation Award Number: DMR-1905559.

Competing financial interests

The authors declare no competing financial interests.

Data availability statement

Data to support the finding of this study are available within the article and its Supplementary Information file. Additional data are available from the corresponding author upon request.

ACKNOWLEDGMENT

We thank Dr. Sarah Perry and Adrian Lorenzana for their critical comments. Research reported in this publication was supported by the Army Research Office Award Number**:** W911NF1910388 and National Science Foundation Award Number: DMR-1905559.

REFERENCES

(1) Lutolf, M. P.; Hubbell, J. A. Synthetic Biomaterials as Instructive Extracellular Microenvironments for Morphogenesis in Tissue Engineering. *Nat. Biotechnol.* **2005**, *23* (1), 47–55. https://doi.org/10.1038/nbt1055.
(2) Tibbitt, M. W.; Anseth, K. S. Hydrogels as Extracellular Matrix Mimics for 3D Cell Culture. *Biotechnol. Bioeng.* **2009**, *103* (4), 655–663. https://doi.org/10.1002/bit.22361.
(3) Slaughter, B. V.; Khurshid, S. S.; Fisher, O. Z.; Khademhosseini, A.; Peppas, N. A. Hydrogels in Regenerative Medicine. *Adv. Mater.* **2009**, *21* (32–33), 3307–3329. https://doi.org/10.1002/adma.200802106.
(4) Kloxin, A. M.; Kloxin, C. J.; Bowman, C. N.; Anseth, K. S. Mechanical Properties of Cellularly Responsive Hydrogels and Their Experimental Determination. *Adv. Mater.* **2010**, *22* (31), 3484–3494. https://doi.org/10.1002/adma.200904179.
(5) Naficy, S.; Brown, H. R.; Razal, J. M.; Spinks, G. M.; Whitten, P. G.; Naficy, S.; Brown, H. R.; Razal, J. M.; Spinks, G. M.; Whitten, P. G. Progress Toward Robust Polymer Hydrogels. *Aust. J. Chem.* **2011**, *64* (8), 1007–1025. https://doi.org/10.1071/CH11156.
(6) K. Piechocka, I.; A. Jansen, K.; P. Broedersz, C.; A. Kurniawan, N.; C. MacKintosh, F.; H. Koenderink, G. Multi-Scale Strain-Stiffening of Semiflexible Bundle Networks. *Soft Matter* **2016**, *12* (7), 2145–2156. https://doi.org/10.1039/C5SM01992C.
(7) Motte, S.; Kaufman, L. J. Strain Stiffening in Collagen I Networks. *Biopolymers* **2013**, *99* (1), 35–46. https://doi.org/10.1002/bip.22133.
(8) Nia, H. T.; Munn, L. L.; Jain, R. K. Physical Traits of Cancer. *Science* **2020**, *370* (6516). https://doi.org/10.1126/science.aaz0868.
(9) Storm, C.; Pastore, J. J.; MacKintosh, F. C.; Lubensky, T. C.; Janmey, P. A. Nonlinear Elasticity in Biological Gels. *Nature* **2005**, *435* (7039), 191–194. https://doi.org/10.1038/nature03521.
(10) Webber, M. J.; Tibbitt, M. W. Dynamic and Reconfigurable Materials from Reversible Network Interactions. *Nat. Rev. Mater.* **2022**, 1–16. https://doi.org/10.1038/s41578-021-00412-x.
(11) Mantooth, S. M.; Munoz-Robles, B. G.; Webber, M. J. Dynamic Hydrogels from Host–Guest Supramolecular Interactions. *Macromol. Biosci.* **2019**, *19* (1), 1800281. https://doi.org/10.1002/mabi.201800281.
(12) Perera, M. M.; Chimala, P.; Elhusain-Elnegres, A.; Heaton, P.; Ayres, N. Reversibly Softening and Stiffening Organogels Using a Wavelength-Controlled Disulfide-Diselenide Exchange. *ACS Macro Lett.* **2020**, *9* (11), 1552–1557. https://doi.org/10.1021/acsmacrolett.0c00718.
(13) Perera, M. M.; Fischesser, D. M.; Molkentin, J. D.; Ayres, N. Stiffness of Thermoresponsive Gelatin-Based Dynamic Hydrogels Affects Fibroblast Activation. *Polym. Chem.* **2019**, *10* (46), 6360–6367. https://doi.org/10.1039/C9PY01424A.
(14) Schild, H. G. Poly(N-Isopropylacrylamide): Experiment, Theory and Application. *Prog. Polym. Sci.* **1992**, *17* (2), 163–249. https://doi.org/10.1016/0079-6700(92)90023-R.
(15) Yoshikawa, H. Y.; Rossetti, F. F.; Kaufmann, S.; Kaindl, T.; Madsen, J.; Engel, U.; Lewis, A. L.; Armes, S. P.; Tanaka, M. Quantitative Evaluation of Mechanosensing of Cells on Dynamically Tunable Hydrogels. *J. Am. Chem. Soc.* **2011**, *133* (5), 1367–1374. https://doi.org/10.1021/ja1060615.
(16) Lee, I.-N.; Dobre, O.; Richards, D.; Ballestrem, C.; Curran, J. M.; Hunt, J. A.; Richardson, S. M.; Swift, J.; Wong, L. S. Photoresponsive Hydrogels with Photoswitchable Mechanical Properties Allow Time-Resolved Analysis of Cellular Responses to Matrix

Stiffening. *ACS Appl. Mater. Interfaces* **2018**, *10* (9), 7765–7776. https://doi.org/10.1021/acsami.7b18302.
(17) FitzSimons, T. M.; Anslyn, E. V.; Rosales, A. M. Effect of PH on the Properties of Hydrogels Cross-Linked via Dynamic Thia-Michael Addition Bonds. *ACS Polym. Au* **2022**, *2* (2), 129–136. https://doi.org/10.1021/acspolymersau.1c00049.
(18) Rosales, A. M.; Rodell, C. B.; Chen, M. H.; Morrow, M. G.; Anseth, K. S.; Burdick, J. A. Reversible Control of Network Properties in Azobenzene-Containing Hyaluronic Acid-Based Hydrogels. *Bioconjug. Chem.* **2018**, *29* (4), 905–913. https://doi.org/10.1021/acs.bioconjchem.7b00802.
(19) Rosales, A. M.; Vega, S. L.; DelRio, F. W.; Burdick, J. A.; Anseth, K. S. Hydrogels with Reversible Mechanics to Probe Dynamic Cell Microenvironments. *Angew. Chem. Int. Ed.* **2017**, *56* (40), 12132–12136. https://doi.org/10.1002/anie.201705684.
(20) Tong, C.; Wondergem, J. A. J.; van den Brink, M.; Kwakernaak, M. C.; Chen, Y.; Hendrix, M. M. R. M.; Voets, I. K.; Danen, E. H. J.; Le Dévédec, S.; Heinrich, D.; Kieltyka, R. E. Spatial and Temporal Modulation of Cell Instructive Cues in a Filamentous Supramolecular Biomaterial. *ACS Appl. Mater. Interfaces* **2022**, *14* (15), 17042–17054. https://doi.org/10.1021/acsami.1c24114.
(21) Mahajan, A.; Singh, A.; Datta, D.; Katti, D. S. Bioinspired Injectable Hydrogels Dynamically Stiffen and Contract to Promote Mechanosensing-Mediated Chondrogenic Commitment of Stem Cells. *ACS Appl. Mater. Interfaces* **2022**, *14* (6), 7531–7550. https://doi.org/10.1021/acsami.1c11840.
(22) Bowser, B. H.; Craig, S. L. Empowering Mechanochemistry with Multi-Mechanophore Polymer Architectures. *Polym. Chem.* **2018**, *9* (26), 3583–3593. https://doi.org/10.1039/C8PY00720A.
(23) Ramirez, A. L. B.; Kean, Z. S.; Orlicki, J. A.; Champhekar, M.; Elsakr, S. M.; Krause, W. E.; Craig, S. L. Mechanochemical Strengthening of a Synthetic Polymer in Response to Typically Destructive Shear Forces. *Nat. Chem.* **2013**, *5* (9), 757–761. https://doi.org/10.1038/nchem.1720.
(24) Fernandez-Castano Romera, M.; Lafleur, R. P. M.; Guibert, C.; Voets, I. K.; Storm, C.; Sijbesma, R. P. Strain Stiffening Hydrogels through Self-Assembly and Covalent Fixation of Semi-Flexible Fibers. *Angew. Chem. Int. Ed.* **2017**, *56* (30), 8771–8775. https://doi.org/10.1002/anie.201704046.
(25) Wang, Y.; Xu, Z.; Lovrak, M.; le Sage, V. A. A.; Zhang, K.; Guo, X.; Eelkema, R.; Mendes, E.; van Esch, J. H. Biomimetic Strain-Stiffening Self-Assembled Hydrogels. *Angew. Chem. Int. Ed.* **2020**, *59* (12), 4830–4834. https://doi.org/10.1002/anie.201911364.
(26) Erk, K. A.; Henderson, K. J.; Shull, K. R. Strain Stiffening in Synthetic and Biopolymer Networks. *Biomacromolecules* **2010**, *11* (5), 1358–1363. https://doi.org/10.1021/bm100136y.
(27) Jaspers, M.; Dennison, M.; Mabesoone, M. F. J.; MacKintosh, F. C.; Rowan, A. E.; Kouwer, P. H. J. Ultra-Responsive Soft Matter from Strain-Stiffening Hydrogels. *Nat. Commun.* **2014**, *5* (1), 5808. https://doi.org/10.1038/ncomms6808.
(28) Middleton, L. R.; Szewczyk, S.; Azoulay, J.; Murtagh, D.; Rojas, G.; Wagener, K. B.; Cordaro, J.; Winey, K. I. Hierarchical Acrylic Acid Aggregate Morphologies Produce Strain-Hardening in Precise Polyethylene-Based Copolymers. *Macromolecules* **2015**, *48* (11), 3713–3724. https://doi.org/10.1021/acs.macromol.5b00797.

(29) Matsuda, T.; Kawakami, R.; Namba, R.; Nakajima, T.; Gong, J. P. Mechanoresponsive Self-Growing Hydrogels Inspired by Muscle Training. *Science* **2019**, *363* (6426), 504–508. https://doi.org/10.1126/science.aau9533.
(30) Zhang, H.; Gao, F.; Cao, X.; Li, Y.; Xu, Y.; Weng, W.; Boulatov, R. Mechanochromism and Mechanical-Force-Triggered Cross-Linking from a Single Reactive Moiety Incorporated into Polymer Chains. *Angew. Chem.* **2016**, *128* (9), 3092–3096. https://doi.org/10.1002/ange.201510171.
(31) Willis-Fox, N.; Rognin, E.; Aljohani, T. A.; Daly, R. Polymer Mechanochemistry: Manufacturing Is Now a Force to Be Reckoned With. *Chem* **2018**, *4* (11), 2499–2537. https://doi.org/10.1016/j.chempr.2018.08.001.
(32) Huo, S.; Zhao, P.; Shi, Z.; Zou, M.; Yang, X.; Warszawik, E.; Loznik, M.; Göstl, R.; Herrmann, A. Mechanochemical Bond Scission for the Activation of Drugs. *Nat. Chem.* **2021**, *13* (2), 131–139. https://doi.org/10.1038/s41557-020-00624-8.
(33) Tran, Y. H.; Rasmuson, M. J.; Emrick, T.; Klier, J.; Peyton, S. R. Strain-Stiffening Gels Based on Latent Crosslinking. *Soft Matter* **2017**, *13* (47), 9007–9014. https://doi.org/10.1039/C7SM01888F.
(34) Scheutz, G. M.; Rowell, J. L.; Wang, F.-S.; Abboud, K. A.; Peng, C.-H.; Sumerlin, B. S. Synthesis of Functional 1,2-Dithiolanes from 1,3-Bis-Tert-Butyl Thioethers. *Org. Biomol. Chem.* **2020**, *18* (33), 6509–6513. https://doi.org/10.1039/D0OB01577F.
(35) Scheutz, G. M.; Rowell, J. L.; Ellison, S. T.; Garrison, J. B.; Angelini, T. E.; Sumerlin, B. S. Harnessing Strained Disulfides for Photocurable Adaptable Hydrogels. *Macromolecules* **2020**, *53* (10), 4038–4046. https://doi.org/10.1021/acs.macromol.0c00604.
(36) Chen, X.; Lawrence, J.; Parelkar, S.; Emrick, T. Novel Zwitterionic Copolymers with Dihydrolipoic Acid: Synthesis and Preparation of Nonfouling Nanorods. *Macromolecules* **2013**, *46* (1), 119–127. https://doi.org/10.1021/ma301288m.
(37) Zhang, X.; Waymouth, R. M. 1,2-Dithiolane-Derived Dynamic, Covalent Materials: Cooperative Self-Assembly and Reversible Cross-Linking. *J. Am. Chem. Soc.* **2017**, *139* (10), 3822–3833. https://doi.org/10.1021/jacs.7b00039.
(38) Chang, C.-C.; Letteri, R.; Hayward, R. C.; Emrick, T. Functional Sulfobetaine Polymers: Synthesis and Salt-Responsive Stabilization of Oil-in-Water Droplets. *Macromolecules* **2015**, *48* (21), 7843–7850. https://doi.org/10.1021/acs.macromol.5b01861.
(39) Ma, J.; Cheng, C.; Sun, G.; Wooley, K. L. Well-Defined Polymers Bearing Pendent Alkene Functionalities via Selective RAFT Polymerization. *Macromolecules* **2008**, *41* (23), 9080–9089. https://doi.org/10.1021/ma802057u.
(40) Zhao, W.; Zhu, Y.; Zhang, J.; Xu, T.; Li, Q.; Guo, H.; Zhang, J.; Lin, C.; Zhang, L. A Comprehensive Study and Comparison of Four Types of Zwitterionic Hydrogels. *J. Mater. Sci.* **2018**, *53* (19), 13813–13825. https://doi.org/10.1007/s10853-018-2535-6.
(41) Richbourg, N. R.; Peppas, N. A. The Swollen Polymer Network Hypothesis: Quantitative Models of Hydrogel Swelling, Stiffness, and Solute Transport. *Prog. Polym. Sci.* **2020**, *105*, 101243. https://doi.org/10.1016/j.progpolymsci.2020.101243.
(42) Flory, P. J. Molecular Theory of Rubber Elasticity. *Polym. J.* **1985**, *17* (1), 1–12. https://doi.org/10.1295/polymj.17.1.
(43) Zhou, H.; Woo, J.; Cok, A. M.; Wang, M.; Olsen, B. D.; Johnson, J. A. Counting Primary Loops in Polymer Gels. *Proc. Natl. Acad. Sci.* **2012**, *109* (47), 19119–19124. https://doi.org/10.1073/pnas.1213169109.

(44) Tsuji, Y.; Li, X.; Shibayama, M. Evaluation of Mesh Size in Model Polymer Networks Consisting of Tetra-Arm and Linear Poly(Ethylene Glycol)s. *Gels* **2018**, *4* (2), 50. https://doi.org/10.3390/gels4020050.
(45) Canal, T.; Peppas, N. A. Correlation between Mesh Size and Equilibrium Degree of Swelling of Polymeric Networks. *J. Biomed. Mater. Res.* **1989**, *23* (10), 1183–1193. https://doi.org/10.1002/jbm.820231007.
(46) Richbourg, N. R.; Ravikumar, A.; Peppas, N. A. Solute Transport Dependence on 3D Geometry of Hydrogel Networks. *Macromol. Chem. Phys.* **2021**, *222* (16), 2100138. https://doi.org/10.1002/macp.202100138.
(47) Liu, Y.; van Steenbergen, M. J.; Zhong, Z.; Oliveira, S.; Hennink, W. E.; van Nostrum, C. F. Dithiolane-Crosslinked Poly(ε-Caprolactone)-Based Micelles: Impact of Monomer Sequence, Nature of Monomer, and Reducing Agent on the Dynamic Crosslinking Properties. *Macromolecules* **2020**, *53* (16), 7009–7024. https://doi.org/10.1021/acs.macromol.0c01031.
(48) Biswas, S.; Yashin, V. V.; Balazs, A. C. Dynamic Behavior of Chemically Tunable Mechano-Responsive Hydrogels. *Soft Matter* **2021**, *17* (47), 10664–10674. https://doi.org/10.1039/D1SM01188J.
(49) Biswas, S.; Yashin, V. V.; Balazs, A. C. Harnessing Biomimetic Cryptic Bonds to Form Self-Reinforcing Gels. *Soft Matter* **2020**, *16* (22), 5120–5131. https://doi.org/10.1039/D0SM00145G.
(50) Yashin, V. V.; Kuksenok, O.; Balazs, A. C. Computational Design of Active, Self-Reinforcing Gels. *J. Phys. Chem. B* **2010**, *114* (19), 6316–6322. https://doi.org/10.1021/jp101009h.

For Table of Contents Only